Stochastic modelling of CO_2 migration in a heterogeneous aquifer

Claude Mügler[1], Emmanuel Mouche[1]

[1]Laboratoire des Sciences du Climat et de l'Environnement (LSCE/IPSL),
CEA-CNRS-UVSQ,
Orme des Merisiers, 91191 Gif-sur-Yvette Cedex, France

Abstract
In this communication, we present the first results of a research program aiming to assess the impact of host-rock heterogeneity on CO_2 plume migration.

Keywords: CO_2, stochastic modelling, heterogeneous aquifer.

Introduction

According to the now classical scenario describing CO_2 sequestration in a geological formation, two periods of the CO_2 plume lifetime may be defined. The first one, which lasts a few years, corresponds to the injection phase and to the vertical migration of the CO_2 plume driven by gravity segregation. During the second period, which can last several hundred of years or even more, the mineral sequestration occurs. Furthermore, the plume possibly migrates through the aquifer cap rock. The plume rise and its final shape depend partly on the permeability of the host formation. At the expected plume lateral scale, kilometric scale, it is probable that permeability will display spatial variability due to rock heterogeneity. It has been shown by Johnson *et al.* [1] that the presence of thin intra-aquifer low-permeability structures such as shale layers has a great influence on the immiscible-plume migration : they maximize the volume where the plume-aquifer interaction takes place and delay the migration of immiscible CO_2. Consequently, these heterogeneities increase the total mass of solubility-trapped CO_2 and the mass percentage of mineral-trapped CO_2.
In this communication, we present the first results of a research program aiming to assess the impact of host-rock heterogeneity on CO_2 plume migration. First, we describe the incompressible two-phase flow model used to simulate the CO_2 injection in the porous media. Several configurations have been used to validate the numerical resolution of the model. Second, we will present the first results of stochastic modelling.

The incompressible two-phase flow model

Classical models of CO_2 injection in a porous media describe the evolution versus time and space of CO_2 saturation [2][3]. In these models, a general mass balance equation for multiphase and multicomponent system is written for each component (CO_2 and water), using the multiphase extension of Darcy's law. The system of equations is then closed with the capillary law. In our model, the mass balance equations for each of the two immiscible fluids (CO_2 and water) are combined in order to obtain a saturation equation and a pressure equation. In the particular case of incompressible fluids and constant porosity, we obtain equations (1) and (2).
In these equations, ω is the porosity, ρ_i and S_i are the density and the saturation of the fluid i (CO_2 or H_2O), respectively. The mass fraction of component CO_2 in liquid phase is noted X_L^{CO2}. The quantities f_i are function of the mobilities of the two fluids according to $f_i=M_i/(M_i+M_j)$, where M_i and M_j are the mobilities of the two fluids. P_c is the capillary pressure, equal to the difference between the CO_2 pressure and the water pressure.

$$\vec{\nabla}.\left[1-\left(1-\frac{\rho_{H_2O}}{\rho_{CO_2}}\right)X_L^{CO_2} f_{H_2O}\right]\vec{u} \tag{1}$$
$$=\left(1-\frac{\rho_{H_2O}}{\rho_{CO_2}}\right)\left\{\omega\frac{\partial}{\partial t}\left[X_L^{CO_2}\left(1-S_{CO_2}\right)\right]-\vec{\nabla}.\left[X_L^{CO_2}M_{H_2O}f_{CO_2}\left(\left(\rho_{H_2O}-\rho_{CO_2}\right)g\overrightarrow{\nabla z}-\overrightarrow{\nabla P_c}\right)\right]\right\},$$

$$\omega\left(1-\frac{\rho_{H_2O}}{\rho_{CO_2}}X_L^{CO_2}\right)\frac{\partial S_{CO_2}}{\partial t}+\omega\frac{\rho_{H_2O}}{\rho_{CO_2}}\left(1-S_{CO_2}\right)\frac{\partial X_L^{CO_2}}{\partial t} \tag{2}$$
$$=-\vec{\nabla}.\left\{\left(f_{CO_2}+\frac{\rho_{H_2O}}{\rho_{CO_2}}X_L^{CO_2}f_{H_2O}\right)\vec{u}+\left(1-\frac{\rho_{H_2O}}{\rho_{CO_2}}X_L^{CO_2}\right)M_{H_2O}f_{CO_2}\left[\left(\rho_{H_2O}-\rho_{CO_2}\right)g\overrightarrow{\nabla z}-\overrightarrow{\nabla P_c}\right]\right\}.$$

The total Darcy velocity, u, is obtained by summing the two mass balance equations and is given by the following expression

$$\vec{u}=-\left(M_{CO_2}+M_{H_2O}\right)\vec{\nabla}P_{CO_2}-\left(M_{CO_2}\rho_{CO_2}+M_{H_2O}\rho_{H_2O}\right)g\vec{\nabla}z+M_{H_2O}\vec{\nabla}P_c \tag{3}$$

Numerical scheme and validation

The partial derivated equations (1) and (2) are solved with the Cast3M code developed at the French atomic energy commission (CEA) (see e.g. [4] and [5] for multiphase flow applications). Due to the strong contrast in the parameters space distribution, we use a Mixed-Hybrid Finite Element (MHFE) formulation. The advection term of Eq.(2) is solved with an upwind scheme.

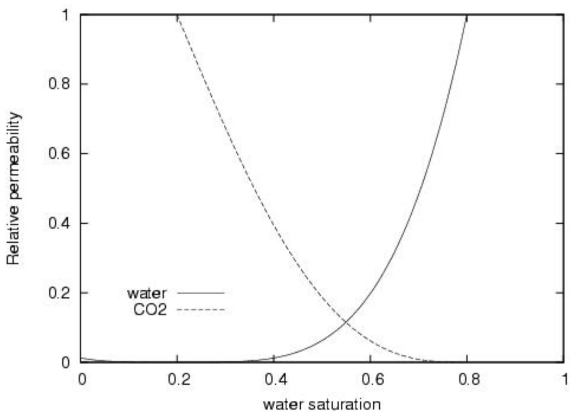

Figure 1 Brooks-Corey permeability-saturation relationships.

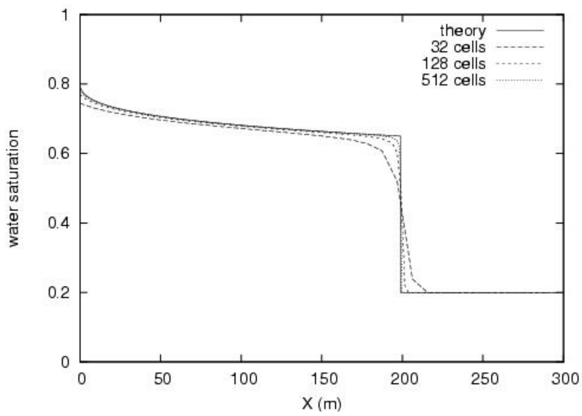

Figure 2 Saturation distribution of water after 1500 days.

When gravity and capillarity effects and CO_2 dissolution are neglected, equations (1) and (2) correspond to the well known Buckley-Leverett problem [6]. This problem describes the instationary displacement of oil by water in a one-dimensional, horizontal system and is a standard method for the verification of multiphase flow processes without capillary pressure effects [7]. The numerical scheme has been validated by comparison of numerical solutions with analytical solutions of this problem. Assuming, for instance, Brooks-Corey permeability-saturation relationships (see Figure 1), Figure 2 shows the saturation distribution of the infiltrating water phase after a period of 1500 days, for different spatial discretizations. Numerical and analytical results are in good agreement. Intercomparisons with GeoSeq test cases [3] are also underway.

Stochastic modelling

The impact of aquifer heterogeneities on the CO_2 plume migration during the injection period is assessed in the framework of stochastic modelling. This approach, classical in subsurface hydrology [8], provides a statistical description of the plume migration in terms of means, variances and eventually probability density functions. Due to heterogeneities, the plume is expected to spread in all directions through permeable flowpaths as for tracer transport in subsurface aquifers. Therefore, statistical quantities of interest are, for instance, space moments of the plume, leading to the macro dispersion tensor, travel time probability density function, … As CO_2 is expected to have a geochemical interaction with rock minerals of the aquifer (trapping, …) quantities describing the plume geometry such as plume volume and surface may be of interest. As a matter of fact, it is assumed in the literature that CO_2 trapping process depends on the mass of dissolved CO_2. This mass is localized inside the plume, and depends therefore on the plume volume, but also outside the plume, this part coming from the plume by molecular diffusion through its surface.

These statistical quantities are computed by Monte-Carlo simulations on large bidimensional grids simulating aquifer vertical sections with an injection point located at the bottom of the aquifer. As this work is in progress we will discuss, from a qualitative point of view, plume spreading in a single realization of an aquifer permeability distribution. First we treat the case of a homogeneous aquifer.

CO_2 migration in a homogeneous aquifer

Simulations of CO_2 migration in a homogeneous aquifer allowed us to characterize the influence of the intrinsic permeability value on the plume migration, and in particular on its spreading. If the permeability is very low, buoyancy effects are negligible around the injection point and the bubble migration is piloted by the injection rate: it grows radially, according to the Buckley-Leverett theory (see Figures 3(a)-(b)). On the contrary, if the permeability is high, buoyancy effects become rapidly predominant (see Figures 3(c)-(d)), and plume migration becomes essentially vertical. In all cases, far enough from the injection well, migration bubble is buoyancy driven.

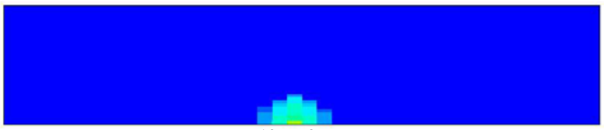

(a) $K=10^{-13}$ m^2, t=0.1 day.

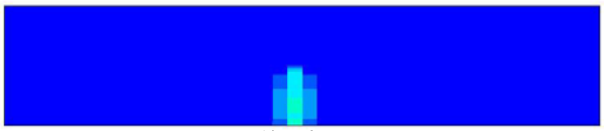

(c) $K=10^{-10}$ m^2, t=0.1 day.

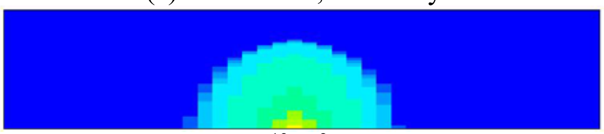

(b) $K=10^{-13}$ m^2, t=1 day.

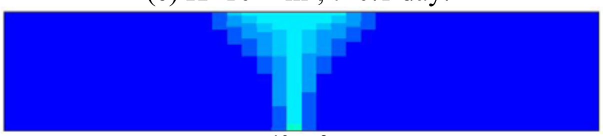

(d) $K=10^{-10}$ m^2, t=1 day.

Figure 3 CO_2 saturation distribution for two different values of aquifer intrinsic permeability K, after 0.1 and 1 day of CO2 injection: (a)-(b) $K=10^{-13}$ m^2 and (c)-(d) $K=10^{-10}$ m^2.

This change of dynamics occurs in a space region where the radial component of the velocity is of the order of magnitude of the buoyancy velocity. This defines, in 2D, a critical radius, $r^*=\alpha Q/K$, origin taken at the injection point, with $\alpha=(\mu_{CO2}/\rho_{CO2})/(2\pi(\rho_{H2O}-\rho_{CO2})gh)$. Q is the injection rate and K the intrinsic permeability. Radial and buoyancy velocities have been estimated according to [9]. For example, for a Q value of 0.32 kg/s and a thickness h equal to1 m, as given in GeoSeq project [3], the radius is approximately equal to 0.01 m for $K=10^{-10}$ m^2 and 10 m for $K=10^{-13}$ m^2. It shows that the ratio of this radius on the aquifer thickness may be a parameter of interest.

CO_2 migration in a heterogeneous aquifer
In this case, CO_2 is injected in a 2D heterogeneous aquifer. We assume that the host-formation intrinsic permeability is described by a lognormal anisotropic random process and we consider a single realization of this permeability distribution. The domain extent is 13 λ_H wide and 50 λ_V high, where λ_H and λ_V are the horizontal and vertical correlation lengths, respectively, with $\lambda_H/\lambda_V=10$ and $\lambda_V=1$ m. The $\log_{10}$ permeability covariance is assumed to be exponential. Two values of mean $\log_{10}$ intrinsic permeability $<\log_{10}K>$ are considered, -10 and -13, each one corresponding to a particular hydrodynamic regime for the homogeneous case (buoyancy driven or injection driven, see preceding section). The $\log_{10}$ standard deviation is equal to one. Figure 4 shows the $\log_{10}$ intrinsic permeability spatial distribution.

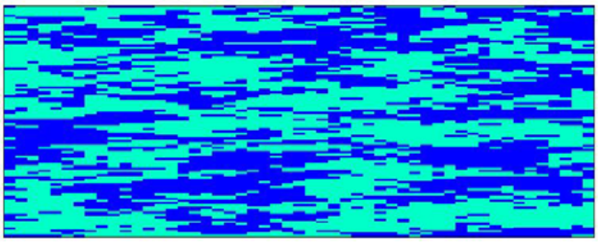

Figure 4 Spatial distribution of $\log_{10}$ intrinsic permeability. Dark and light zones correspond to $\log_{10}$ permeability values less and greater than the mean value, respectively.

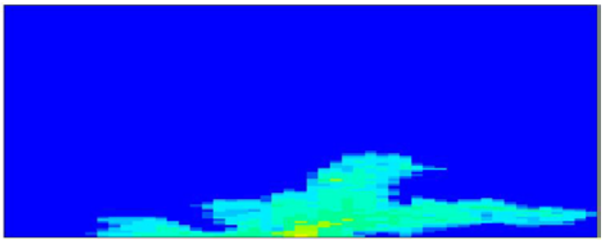

(a) $<\log_{10}K> = -13$, t = 2 days.

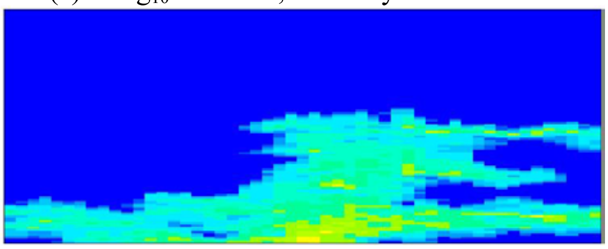

(b) $<\log_{10}K> = -13$, t = 8 days.

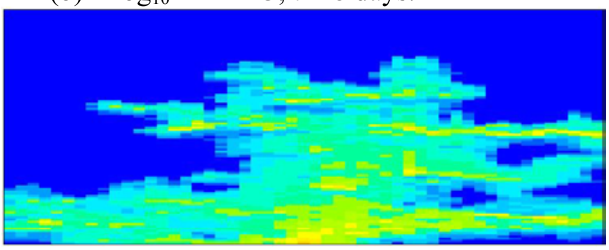

(c) $<\log_{10}K> = -13$, t = 22 days.

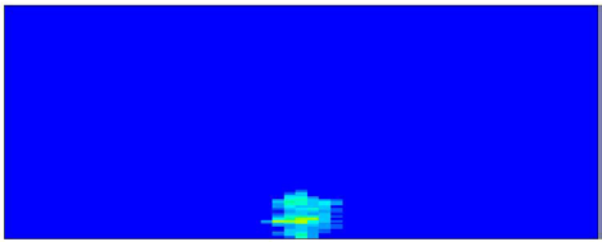

(d) $<\log_{10}K> = -10$, t = 0.2 day.

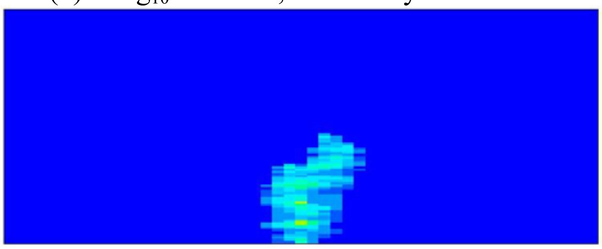

(e) $<\log_{10}K> = -10$, t = 0.5 day.

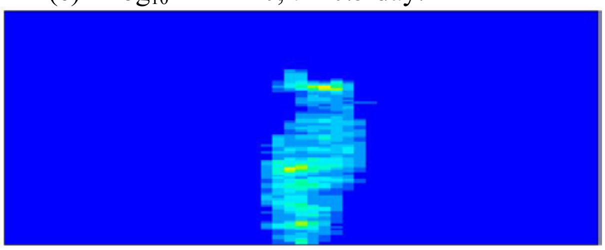

(f) $<\log_{10}K> = -10$, t = 0.9 day.

Figure 5 CO_2 saturation distribution for two values of mean $\log_{10}$ intrinsic permeability and at different times: (a)-(c) $<\log_{10}K> = -13$ and t = 2, 8 and 22 days; (d)-(f) $<\log_{10}K> = -10$ and t = 0.2, 0.5 and 0.9 day.

Figures 5(a)-(c) and 5(d)-(f) show the plume distribution at three times for the two different values of mean $\log_{10}$ intrinsic permeability previously used in the homogeneous case. The three times are

different as the mean $\log_{10}$ permeabilities are different. A comparison of timescales is not straightforward, e.g. given by the ratio of $\log_{10}$ intrinsic permeabilities: in the buoyancy driven case the mean velocity is vertical and constant and in the injection driven case the velocity is radial and decreases with distance to the injection point. Figures 5(a)-(c), injection driven case, show that, in a first step, the plume spreads radially through permeable flowpaths and reaches rapidly the domain lateral limits, and diffuses, in a second step in the low permeable strata. In the buoyancy driven case (see Figures 5(d)-(f)), the plume rises vertically, in a quasi 1D migration, through strata distribution. Due to the small extent of the injection zone there is no vertical spreading. To see this spreading the injection zone should be much larger than the horizontal correlation length. These different types of spreadings may be quantified by their respective macro dispersion tensors. This transport parameter is obtained from a moment analysis of the CO_2 saturation spatial distribution [8].
Concerning the surface of the CO_2 plume one sees from Figures 5 (a)-(f) that a low permeability (injection driven case) enhances the expansion of the surface. For the volume there seems that many parameters intervene in the volume increase and the understanding of this quantity is not clear yet.
One of the first outcomes of this preliminary analysis is that in the buoyancy driven case the plume should occupy the top of the aquifer only. At the contrary in the injection driven case the plume should invade all the aquifer. This shows the importance of the injection procedure.

Conclusion

We show in this paper that the CO_2 plume migration in a heterogeneous aquifer during injection depends strongly on the mean permeability. For low values, the mean migration is radial and macro dispersion seems to be similar to a single phase injection in a multiphase reservoir : the plume exhibits fingers moving radially in permeable flowpaths. For high values, buoyancy is predominant: the mean migration is vertical and macro dispersion should occur only vertically. The transition between these two regimes depends on a critical radius. These results need to be confirmed by Monte-Carlo simulations and a moment analysis of CO_2 saturation distribution. One of the final objectives of this work is to define equivalent migration parameters for large scale simulations, corresponding to those that would be obtained for an equivalent homogeneous media.

Acknowledgements

This study is supported by the CNRS, as part of the “Mineral trapping of CO2” project of the ACI Energy.

References

[1] Johnson JW, Nitao JJ, Steefel CI, Knauss KG. Reactive transport modeling of geologic CO_2 sequestration in saline aquifers: the influence of intra-aquifer shales and the relative effectiveness of structural, solubility, and mineral trapping during prograde and retrograde sequestration. Proceedings of the First National Conference on Carbon Sequestration.Washington DC, May 14-17; 2001.
[2] Chavent G, Jaffre J. Mathematical models and finite elements for reservoir simulation. North-Holland, Vol. 17; 1986.
[3] Pruess K, Garcia J, Kovscek T, Oldenburg C, Rutqvist R, Steefel C, Xu T. Intercomparison of numerical simulation codes for geologic disposal of CO_2, LBNL-51813 report; 2002.
[4] Le Potier C, Mouche E, Genty A, Benet LV, Plas F. Mixed Hybrid Finite Element formulation for water flow in unsaturated porous media. Computational Methods in Water Resources XII, Vol. 1. Computational Mechanics Publications; 1998.
[5] Genty A, Le Potier C, Renard P. Two-phase flow upscaling with heterogeneous tensorial relative permeability. Computational Methods in Water Resources XIII, Vol. 2. Computational Mechanics Publications; 2000.
[6] Buckley SE, Leverett MC. Mechanism of fluid displacement in sands. Trans. Am. Inst. Mineral Metall. Eng. 1942; 146:107-116.

[7] Helmig R. Multiphase flow and transport processes in the subsurface. Springer-Verlag Berlin Heidelberg; 1997.
[8] Gelhar LW. Stochastic subsurface hydrology. Prentice Hall, Englewood Cliffs. New Jersey; 1993.
[9] Saripalli P, McGrail P. Semi-analytical approaches to modelling deep well injection of CO_2 for geological sequestration. Energy Convers Mgmt 2002; 43:185-198.